Excited-State Tautomerization Dynamics of 7-Hydroxyquinoline in β-Cyclodextrin

Han Jung Park, Oh-Hoon Kwon, Chil Seong Ah,† and Du-Jeon Jang*

School of Chemistry, Seoul National University, NS60, Seoul 151-742, Korea

Received: July 19, 2004; In Final Form: October 14, 2004

The excited-state tautomerization dynamics of 7-hydroxyquinoline encapsulated in β-cyclodextrin is compared with that in pure water by measuring isotope-dependent fluorescence kinetics as well as absorption and emission spectra. The normal species tautomerizes stepwise via forming anionic intermediate species in both systems. However, the enol-deprotonation time (40 ps in water) becomes as large as 170 ps whereas the imine-protonation time of the anionic intermediate (160 ps in water) becomes as short as 85 ps in β-cyclodextrin. The slow formation and the fast decay of the anionic species are attributed to the unstability of the charged species in hydrophobic cages. Encapsulation can be utilized to enhance fluorescence enormously and to accelerate selective reactions by retarding other processes.

Introduction

Proton transfer has been attracting considerable attention because it plays a key role in a wide variety of biological and chemical phenomena.[1−8] In particular, proton transfer in water is fundamentally very important but enormously complicated. Recent interest is on the dissociation dynamics of a proton from an acid[9−13] and on the dispersion dynamics of hydrated proton clusters in bulk solvents.[14−17] The proton-transfer dynamics is determined by the size, structure, and motion of a solvent cluster as well as by the nature of a prototropic group[9−12,18−24] whereas proton migration is controlled by solvent structural dynamics.[14−17] The dynamics and mechanism of excited-state proton transfer (ESPT) to water have been often investigated with photoacids.[25−27] The most important feature controlling the extremely fast excited-state proton transfer into an aqueous medium is the formation of a specifically structured water cluster.[5,9] Water clusters having 4 ± 1 molecules have been suggested to be the proton acceptors of photoacids.[28] Proton-transfer studies employing various naphthol derivatives have indicated that the apparent sizes of the accepting water clusters also depend on the nature of the proton donors.[29,30] In the case where two groups with opposite p*K** tendencies exist in a molecule, a photon may initiate protonation and deprotonation to yield a tautomeric species in water. Proton transfers for this type of molecules, having as many as four potential wells in S_1, are interesting to study because they may serve as experimental models for the migration and pumping of protons in biological systems.[31]

In this regard, hydroxyquinolines and their derivatives, having two prototropic enol and imino groups, are extensively explored.[19,20,32−47] The enol and imino groups of 3-, 6-, and 7-hydroxyquinoline (7HQ) become much more acidic and basic, respectively, in S_1 than in S_0. Utilizing these large p*K* differences, many groups have been studying hydroxyquinolines to understand the deprotonation of the enol group and the protonation of the imino group in S_1 and their reverse processes in S_0. 7HQ in nonaqueous protic solvents is known to form a hydrogen-bonding chain, through which proton relay can take place.[19,33−36] However, 7HQ, as well as 3- and 6-hydroxyquinoline, undergoes tautomerization stepwise in water via forming intermediate prototropic species.[20,43,44] The individual catalytic roles of H_2O, H_3O^+, and OH^-, as well as the involvement of solvent structural dynamics in the deprotonation of the enol group and in the migration of a hydrated proton cluster, have been reported in the tautomerization reactions of 3- and 6-hydroxyquinoline.[20,44] 7HQ in water exists as one of four prototropic species: a normal molecule (**N**), an imine-protonated cation (**C**), an enol-deprotonated anion (**A**), and an imine-protonated and enol-deprotonated zwitterionic tautomer (**T**), as described in Figure 1. Equilibrium constants[42] indicate that 7HQ in water exists mostly as **N** (67%) and **T** (29%) with minor species of **C** (3%) and **A** (1%) at pH 7.

However, 7HQ encapsulated in β-cyclodextrin (β-CD) exists almost exclusively as **N** at pH 7 (vide infra). Thus, we can initiate the excited-state tautomerization of **N*** by exciting **N** selectively at 315 nm. Because proton transfers are highly sensitive to environment, they are affected markedly by microheterogeneous structures having restricted microenvironment or cavities.[49,50] Cyclodextrins (CDs) have attracted long-standing interests in the field of artificial catalysts.[50−57] Their cone-shaped cages consist of α,D-glucose subunits and possess nonpolar cavities with polar rims containing primary and secondary hydroxyl groups. CDs are soluble in water and their hydrophobic cavities are capable of sequestering a variety of polar and nonpolar compounds and controlling the chemistry of reactive molecules. Three different types of water are generally assumed to exist in aqueous CD solutions: water inside the cavity, water near the rims, and bulk water.[51] A number of studies have reported the effects of micelles and CDs on proton transfers to shed light on the influences of lipophilic environment in processes.[45,58,59]

When 7HQ is encaged in the hydrophobic cavity of a β-CD derivative in water, the enol group is reported to locate at the primary rim while the imino group locates at the secondary rim.[45] Although the photoinduced double proton transfer of 7HQ is reported to be markedly slower than that in pure water,[45] the detailed tautomerization mechanism, as well as the specific influences of β-CD on the proton-transfer dynamics, has not been revealed yet. In this paper, we will show that the inclusion

* To whom correspondence should be addressed. E-mail: djjang@snu.ac.kr.
† Present address: Korea Research Institute of Standards and Science, Daejeon 305-600, Korea.

10.1021/jp046817m CCC: $30.25
Published on Web 02/10/2005

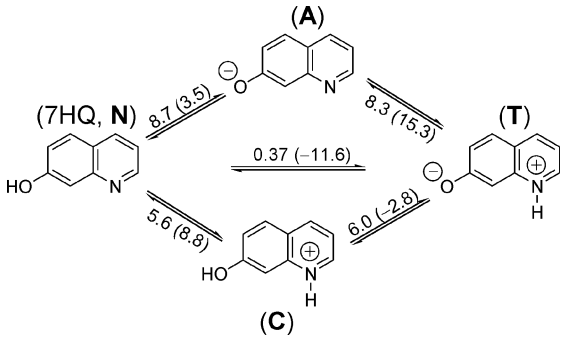

Figure 1. Equilibria among the prototropic species of 7HQ in water. The indicated values of pK (pK*) are taken from ref 42.

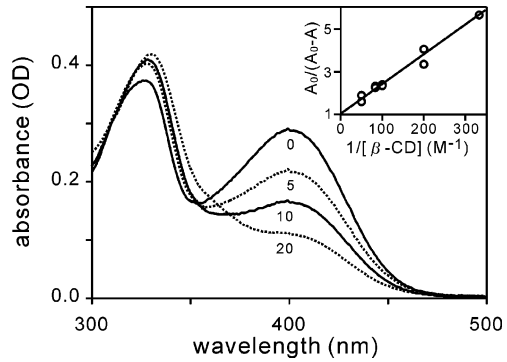

Figure 2. Absorption spectra of 0.1 mM 7HQ in water having the indicated millimolar concentrations of β-CD. Inset: $A_0/(A_0 - A)$ at 405 nm as a function of $[\beta\text{-CD}]^{-1}$ (circles) and the best-fitted linear plot (line), yielding 88 M^{-1} for the association constant of 7HQ with β-CD.

of 7HQ in β-CD having the cavity diameter of 7.8 Å retards the OH-deprotonation of **N*** by four times whereas it accelerates the N-protonation of **A*** by two times.

Experimental Section

Materials. 7HQ (99%) purchased from Acros and β-CD purchased from Aldrich were used without further purification. Aqueous solutions of 7^1HQ and 7^2HQ were prepared by dissolving 7HQ in triply distilled water and in ^2H_2O (isotopic purity ≥99.9%) purchased from Sigma, respectively. Aqueous 7HQ solutions were adjusted to pH 7.0 by adding aqueous solutions of HCl and NaOH. Results presented hereafter were obtained using aqueous 7HQ solutions of 0.1 mM at pH 7.0 and at room temperature unless specified otherwise.

Measurements. Absorption spectra were obtained using a UV/vis spectrometer (Scinco, S-3100). Fluorescence spectra were obtained by using a home-built fluorometer consisting of a 75-W Xe lamp (ARC, XS 432), 0.15-m and 0.30-m monochromators (ARC, Spectrapro 150 and 300), and a photomultiplier tube (ARC, PD 438). Fluorescence spectra were not corrected for the wavelength-dependent sensitivity variation of the detector. An actively/passively mode-locked 25-ps Nd:YAG laser (Quantel, YG 701) and a 10-ps streak camera (Hamamatsu, C2830) attached to a CCD detector (Princeton Instruments, RTE128H) were employed for excitation and detection, respectively. Samples were excited with 315-nm pulses generated through a Raman shifter filled with methane at 15 atm and pumped by the fourth-harmonic pulses (266 nm) of the laser although samples at pH values of 3 and 11 were excited by the third-harmonic pulses (355 nm) of the laser. Emission wavelengths were selected by combining band-pass and cutoff filters. Fluorescence kinetic parameters were extracted by fitting measured kinetic profiles to computer-simulated curves of exponential rise followed by exponential decay convoluted with instrumental response functions.

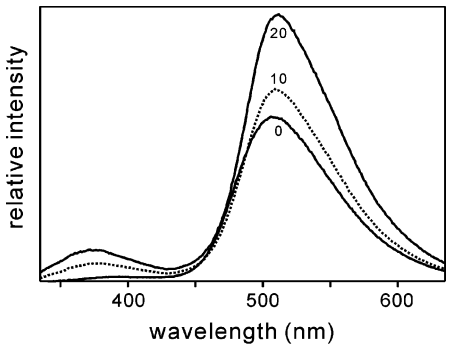

Figure 3. Emission spectra of 0.1 mM 7HQ in water having the indicated millimolar concentrations of β-CD after excitation at 320 nm.

Results and Discussion

UV/Vis Absorption Spectra. The characteristic absorption bands having the peaks at 330 and 405 nm in Figure 2 are due to **N** and **T**, respectively, while the weak absorption bands of **C** and **A** at 350 and 360 nm, respectively, are buried under the two major bands at pH 7.[38,41,42] The absorbance of **T** at 405 nm decreases drastically with β-CD addition whereas the absorbance of **N** at 330 nm tends to increase. These spectral changes suggest that the equilibrium between **N** and **T** shifts to **N** enormously in the cages of β-CD. It is inferred that the zwitterionic species of **T** is much more unstable than the neutral species of **N** in the hydrophobic interior of β-CD.

$$\mathbf{N} \rightleftharpoons \mathbf{T} \qquad (K_1 = 0.43) \tag{1}$$

$$\mathbf{T} + \beta\text{-CD} \rightleftharpoons \mathbf{N}/\beta\text{-CD} \qquad (K_2 = 88\ M^{-1}) \tag{2}$$

While the equilibrium constant of eq 1 is reported by Mason et al.,[42] that of eq 2 for the conversion of **T** to **N** with inclusion has been obtained to be 88 M^{-1} by plotting the relation of eq 3[60] in the inset of Figure 2.

$$\frac{A_0}{A_0 - A} = \frac{\epsilon_M}{\epsilon_M - \epsilon_C}\left(\frac{1}{K_2[\beta\text{-CD}]} + 1\right) \tag{3}$$

A_0 denotes absorbance at 405 nm without β-CD presence and ϵ_M and ϵ_C are the molar extinction coefficients of 7HQ and 7HQ/β-CD, respectively, at 405 nm.[42] The linearity of the plot implies that 7HQ and β-CD form 1:1 inclusion complexes.[45,60] By combining eqs 1 and 2, we can obtain eq 4.

$$\mathbf{N} + \beta\text{-CD} \rightleftharpoons \mathbf{N}/\beta\text{-CD} \qquad (K_3 = 38\ M^{-1}) \tag{4}$$

The equilibrium constant of eq 4 indicates that only the 40% of **N** molecules in the aqueous solutions of 0.1 mM 7HQ and 20 mM β-CD, which were employed for fluorescence kinetic measurements, are encapsulated in β-CD (vide infra). It is noteworthy that the absorption increase at 330 nm is only one-fourth of the absorption decrease at 405 nm by the presence of 20-mM β-CD. The absorption of **T** to higher excited states makes the absorption change at 330 nm smaller than that at 405 nm. This indicates that our irradiation at 315 nm for fluorescence kinetic measurements excites not only **N** but also **T**.

Fluorescence Spectra. The emission spectrum, with excitation at 315 nm, of aqueous 7HQ without β-CD shows only the dominant fluorescence band of **T*** at 510 nm (Figure 3),

suggesting that facile ESPT takes place.[38,39,42] In the presence of β-CD, however, excitation at 315 nm gives birth to prominent **N*** fluorescence at 380 nm as well as **T*** fluorescence at 510 nm. Fluorescence bands from possible intermediate species of **C*** and **A***, expected at 450 and 490 nm, respectively,[38,41,42] are not observable in the static spectra of Figure 3 at any concentrations of β-CD. The intensity of **N*** as well as that of **T*** tends to increase with the increase of [β-CD]. This indicates that 7HQ becomes more fluorescent in β-CD cages. Furthermore, the addition of β-CD induces the hypsochromic shift of **N*** emission and the bathochromic shift of **T*** emission. Because 7HQ is encapsulated into the hydrophobic cavity of β-CD, the lowest $^1(\pi,\pi^*)$ transition of **N** shifts to the blue. On the other hand, the solvatochromism of **T*** emission to the red with the decrease of the medium polarity can be explained with the different electronic structures of **T** and **T***. **T** has zwitterionic character with large charge separation whereas **T*** undergoes rapid electronic rearrangement to possess ketonic character, causing the dipole moment of **T*** to be much smaller than that of **T**. Thus, **T** becomes more unstable whereas **T*** becomes more stable in the hydrophobic interior of β-CD than in water, resulting the red shift of **T*** fluorescence in the molecular cages. Moreover, the bathochromic shift is more profound at 470 nm, implying that the contribution of intermediate emission is reduced by the presence of β-CD. This suggests that 7HQ prototropic species are modified energetically in the cavities to show different ESPT dynamics from that in neat water (vide infra). It is noteworthy that **T*** fluorescence following the direct excitation of **T** at 405 nm in the presence of β-CD is spectrally identical with that in neat water. This indicates that the prototropic species of encapsulated 7HQ is **N**. **T** existing in the aqueous solution of β-CD is resident outside β-CD without forming complexes. Note that the increment of **N*** fluorescence is much greater than the population increment of **N** by the presence of β-CD. This implies that the profound increase of **N*** emission reflects not only population increase but also lifetime increase owing to retarded ESPT (vide infra).

Tautomerization Dynamics of Aqueous N*. The excitation of aqueous **N** without β-CD at pH 7 gives three distinctive fluorescence kinetic profiles of **N*** at 360 nm, intermediate species at 450 nm, and **T*** at 600 nm (Figure 4). It must be pointed out that irradiation at 315 nm gives not only the excitation of **N** but also the excitation of **T**, as discussed with the UV/vis spectra of Figure 2. Hence, the instant rise of **T*** emission originates from the direct excitation of **T** at the ground state. Owing to spectral congestion, kinetics monitored at 450 nm contains the interference fluorescence of **N*** and **T*** in addition to intermediate fluorescence. While the rise time of the intermediate (40 ps) is the same as the decay time of **N***, the lifetime of the intermediate (160 ps) is the same as the rise time of **T*** (Table 1). This designates that ESPT takes place stepwise via forming intermediate species. On the other hand, **C*** at pH 3 decays in 23 ps and **A*** at pH 11 fluoresces on the time scale of 160 ps, clarifying that **N*** in water undergoes excited-state tautomerization stepwise via forming **A*** ($pK_a^* = 0.3$) as the intermediate species.[67] **A***, rather than **C***, as the reaction intermediate can be rationalized with principles involved in intramolecular electronic charge transfers. The intermolecular proton-transfer rates of photoacids and photobases are closely related to the excess stabilization energies of respective conjugates that render proton transfers to be highly exothermic and facile. Because the lowest absorption energy of **A** (27780 cm^{-1}) is smaller than that of **C** (28990 cm^{-1}), the deprotonation of the enol group in the precursor of **N*** is expected to be more exothermic and more facile than the protonation of the imino group. Interestingly, 3- and 6-hydroxyquinoline are already reported to undergo tautomerization consecutively via forming anionic intermediate.[20,43,44] The tautomerization of aqueous 7HQ is reported to take place stepwise without the determination of the intermediate.[32,38] Additionally, some kinetic parameters reported differ from those obtained in this work. These differences can be attributed to the limited temporal resolution of the previous measurements.[38]

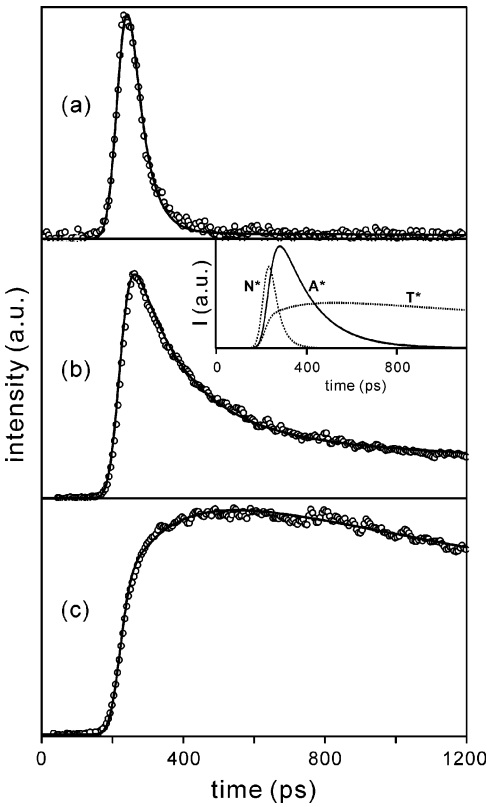

Figure 4. Fluorescence kinetic profiles (circles) and best-fitted curves (lines) of 0.1 mM 7HQ in water, excited at 315 nm and monitored at 360 ± 5 (a), 450 ± 5 (b), and 600 ± 20 nm (c). Inset: The emission kinetic profiles of the respectively indicated species employed to simulate the best-fitted kinetic curve at 450 nm.

The kinetic isotope effect (KIE) of enol deprotonation for **N*** is 2.1 while the KIE of imine protonation for **A*** is 2.4 (Table 2). These KIE values are larger than the KIE (1.4) of proton migration in water originating from the cleavage of hydrogen bonds. Both the deprotonation of the enol group and the protonation of the imino group are slower than either the formation or the dissociation of water clusters. Thus, considering the rates and the KIEs, we suggest that the proton transfers of 7HQ prototropic species are activated processes having tunnel effects along proton coordinates (vide infra).

Tautomerization Dynamics of N* in β-CD Cages. Following the excitation of **N** in aqueous solutions of 20 mM β-CD, **N*** fluorescence decays in 93 ps to give birth to **A*** fluorescence, which decays on the time scale of 130 ps to feed **T*** fluorescence (Figure 5 and Table 1). On the other hand, the lifetime of **T*** is as long as 4200 ps. Because 40% and 60% of **N** molecules in the solutions are enclosed in β-CD and free in bulk water, respectively, at the moment of excitation, the time constants of 7HQ prototropic species encapsulated in β-CD should be extracted from the above apparent time constants by employing the global analysis of double decays.[61,62] Thus, upon absorption of a photon, 7HQ in β-CD undergoes the excited-state deprotonation of the enol group on the time scale of 170 ps to form

TABLE 1: Isotope-Dependent Kinetic Constants of 7HQ Fluorescence in Neutral Water with and without β-CD

isotope[a]	[β-CD] (mM)	λ_{em} (nm)	time constant[b] (ps)
^{1}H	0	360	**40**
		450	40 (43%)[c] + (−**40**)**160** (**45%**) + {2800 (60%) + (−160)2800 (40%)} (12%)
		600	2800 (60%) + (−**160**)**2800** (**40%**)
^{1}H	20	360	**93**
		450	93 (43%) + (−**93**)**130** (**45%**) + {2800 (41%) + (−85)4200 (59%)} (12%)
		600	2800 (41%) + (−**85**)**4200** (**59%**)
^{2}H	0	360	**83**
		450	83 (43%) + (−**83**)**380** (**45%**) + {9200 (55%) + (−380)9200 (45%)} (12%)
		600	9200 (55%) + (−**380**)**9200** (**45%**)
^{2}H	20	360	**260**
		450	260 (43%) + (−**260**)**270** (**45%**) + {9200 (30%) + (−270)16000 (70%)} (12%)
		600	9200 (30%) + (−**270**)**16000** (**70%**)

[a] Isotope of protic hydrogen. [b] Negative and positive values indicate rise and decay time constants, respectively. [c] Amplitude percentage of each component.

TABLE 2: Proton-Transfer and Relaxation Times of Excited 7HQ Prototropic Species in Water at pH 7

species	encapsulated in β-CD	process	time (ps) with ^{1}H	time (ps) with ^{2}H	KIE
N*	no	OH-deprotonation	40[a]	83	2.1
	yes		170	530	3.1
A*	no	N-protonation	160[b]	380	2.4
	yes		85	100	1.2
T*	no	relaxation	2800	9200	3.3
	yes		6300	26000	4.1

[a] The OH-deprotonation time of **C*** at pH 3 is 23 ps. [b] The N-protonation time of **A*** at pH 11 is also 160 ps.

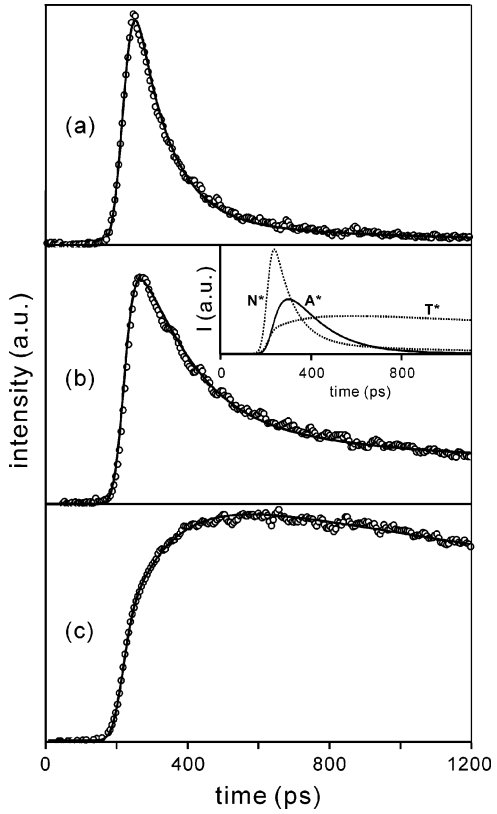

Figure 5. Fluorescence kinetic profiles (circles) and best fitted curves (lines) of 0.1 mM 7HQ in water having 20 mM β-CD, excited at 315 nm and monitored at 360 ± 5 (a), 450 ± 5 (b), and 600 ± 20 nm (c). Inset: The emission kinetic profiles of the respectively indicated species employed to simulate the best-fitted kinetic curve at 450 nm.

intermediate **A***, which experiences the excited-state protonation of the imino group within 85 ps to produce **T*** (Table 2). The retardation of enol deprotonation and the acceleration of imine protonation explain now why **N*** fluorescence increases whereas **A*** fluorescence decreases with the increase of [β-CD] in Figure 3 (vide supra). The retardation of deprotonation is also reported in 1-naphthol complexed with β-CD.[51] It is noteworthy that the fraction of instant-rising **T*** is smaller in β-CD solutions than in neat water. This is consistent with the previous suggestion that the equilibrium between **N** and **T** shifts toward **N** enormously in β-CD cages (Figure 2). The relaxation time of **T*** is elongated from 2.8 to 6.3 ns by encapsulation to yield strongly enhanced fluorescence. The tightly confining geometry of the molecular cage decreases the radiationless relaxation processes of **T*** to extend the fluorescence lifetime of the encaged species.

The KIE value of **N*** deprotonation increases by 47% whereas that of **A*** protonation decreases by 50% with encapsulation. Both processes of **N*** deprotonation and **A*** protonation in water occur through the barriers of proton-transfer coordinates. The KIE values in β-CD suggest that encapsulation in the hydrophobic interior raises the barrier of deprotonation for the formation of an ionic species. The KIE of 1-naphthol deprotonation is also reported to increase gradually with the fractional increase of methanol in water.[63] On the other hand, encapsulation in the hydrophobic interior removes the barrier of protonation for the transformation of an anion to a zwitterion. The activation-controlled reaction of **A*** protonation in water becomes almost solvent-controlled in β-CD. Although the KIE of 1-naphthol relaxation is reported to be as large as 4.4,[65,66] quite intriguing is that the largest KIE of 4.1 is obtained with **T*** relaxation. **T*** does not go through reverse proton-transfer owing to its large stabilization energy having increased basicity at the nitrogen atom and increased acidity at the oxygen atom. Therefore, the large KIE value suggests that the nonradiative relaxation rate of **T*** is mostly determined by internal conversion and intersystem crossing associated with N−H vibrations. Not only tunneling effects but also quantum effects in the vibrational motions of N−H coordinates are reported to lead large KIEs in the water-assisted tautomerization of a formamidine−water complex.[68] In addition, KIE for the fluorescence decay of a 7-azaindole derivative possessing N−H vibrations is reported to be 2.1.[69] Due to the lack of information at this stage, however, more vigorous insight on the large KIE of **T*** relaxation should be left for future work.

Figure 6 summarizes that because ionic **A*** becomes more unstable in a hydrophobic cage than in water, the deprotonation of **N*** is energetically unfavorable by encapsulation to show the small rate constant of (170 ps)$^{-1}$ with a reduced value of K_a*. Because the photoacidity of **N*** ($pK_a^* = 0.3$)[67] is much stronger than that of 2-naphthol ($pK_a^* = 2.8$),[9] the roles of water clusters as proton acceptors are less important for **N*** depro-

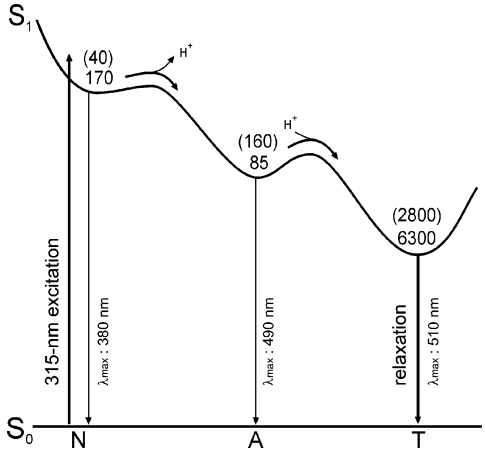

Figure 6. Proton-transfer and relaxation times in picoseconds of photoexcited 7HQ encapsulated in aqueous β-CD. Those in neat water are shown in parentheses.

tonation.[70] Thus, the retardation (by four times) of enol deprotonation to form **A*** by inclusion in β-CD is thought to result mainly from altered acid−base energetics caused by modified electronic structures. The retardation and increased KIE of **N*** deprotonation resulting from the decrease of K_a* in β-CD are in accordance with the picture of a free-energy relationship for an activated ESPT process.[63,64] Energetic modification is expected to be more dominant in the imine protonation of **A***. **T*** is supposed to be of lower energy in β-CD than in water due to its increased ketonic character. Therefore, the imine protonation of **A*** to produce **T*** would be more exoergic and facile. However, the protonation is accelerated less significantly (47%) than the retardation of **N*** deprotonation. These imply that the formation of a water cluster having a finite number of molecules to donate a proton is essential for the protonation of **A*** because the quinoline moiety of 7HQ is surrounded by the hydrophobic interior of β-CD. Furthermore, the KIE value of **A*** protonation falls off from 2.4 to 1.2 by inclusion in β-CD. This trend also suggests a mechanistic switch of activation-controlled protonation into solvation-controlled proton association. Therefore, the acceleration of **A*** protonation caused by acid−base energetic alteration in the hydrophobic cages seems to be superimposed by the deceleration by the structural perturbations of proton-donating water clusters. On the other hand, an inclusion complex of 7HQ with β-CD is a system having a limited number of water molecules. The relaxation time of **T*** increases by a factor of 2.3 with inclusion. This retardation strongly depends on the restricted vibrational motions of N−H and the slow solvation processes of highly constrained water molecules. In conclusion, encapsulation in cages can be utilized to enhance fluorescence enormously and to accelerate selective reactions by retarding other processes.

Acknowledgment. We are greatly in dept to Professor Ehud Pines at the Ben-Gurion University of the Negev for fruitful discussion. This work was supported by the Korea Research Foundation Grant (2003-041-C00151). D.-J.J., H.J.P., and O.-H.K. also acknowledge the Strategic National R&D, the Brain Korea 21, and the Young-Do Foundation, respectively.

References and Notes

(1) Rini, M.; Magnes, B.-Z.; Pines, E.; Nibbering, E. T. J. *Science* **2003**, *301*, 349.
(2) Tanner, C.; Manca, C.; Leutwyler, S. *Science* **2003**, *302*, 1736.
(3) Ceulemans, J. *Acc. Chem. Res.* **2002**, *35*, 523.
(4) Kirby, A. J. *Acc. Chem. Res.* **1997**, *30*, 290.
(5) Douhal, A.; Lahmani, F.; Zewail, A. H. *Chem. Phys.* **1996**, *207*, 477.
(6) Catalán, J.; Pérez, P.; del Valle, J. C.; de Paz, J. L. G.; Kasha, M. *Proc. Natl. Acad. Sci. U.S.A.* **2002**, *99*, 5793.
(7) Kim, S.; Kim, T.-G.; Ah, C. S.; Kim, K.; Jang, D.-J. *J. Phys. Chem. B* **2004**, *108*, 880.
(8) Kwon, O.-H.; Lee, Y.-S.; Park, H. J.; Kim, Y.; Jang, D.-J. *Angew. Chem., Int. Ed.* **2004**, *43*, 5792.
(9) Tolbert, L. M.; Solntsev, K. M. *Acc. Chem. Res.* **2002**, *35*, 19.
(10) Solntsev, K. M.; Tolbert, L. M.; Cohen, B.; Huppert, D.; Hayashi, Y.; Feldman, Y. *J. Am. Chem. Soc.* **2002**, *124*, 9046.
(11) Solntsev, K. M.; Huppert, D.; Agmon, N. *Phys. Rev. Lett.* **2001**, *86*, 3427. Solntsev, K. M.; Huppert, D.; Agmon, N. *J. Phys. Chem. A* **2001**, *105*, 5868. Solntsev, K. M.; Agmon, N. *Chem. Phys. Lett.* **2000**, *320*, 262.
(12) Cohen, B.; Huppert, D.; Agmon, N. *J. Phys. Chem. A* **2001**, *105*, 7165.
(13) Ando, K.; Hynes, J. T. *J. Phys. Chem. B* **1997**, *101*, 10464.
(14) Marx, D.; Tuckerman, M. E.; Hutter, J.; Parrinello, M. *Nature* **1999**, *397*, 601.
(15) Tuckerman, M. E.; Marx, D.; Klein, M. L.; Parrinello, M. *Science* **1997**, *275*, 817.
(16) Kornyshev, A. A.; Kuznetsov, A. M.; Spohr, E.; Ulstrup, J. *J. Phys. Chem. B* **2003**, *107*, 3351.
(17) Walrafen, G. E.; Chu, Y. C.; Carlon, H. R. *J. Phys. Chem. A* **2002**, *106*, 933.
(18) Yu, W.-S.; Cheng, C.-C.; Cheng, Y.-M.; Wu, P.-C.; Song, Y.-H.; Chi, Y.; Chou, P.-T. *J. Am. Chem. Soc.* **2003**, *125*, 10800.
(19) Kwon, O.-H.; Doo, H.; Lee, Y.-S.; Jang, D.-J. *ChemPhysChem* **2003**, *4*, 1079.
(20) Kim, T.-G.; Kim, Y.; Jang, D.-J. *J. Phys. Chem. A* **2001**, *105*, 4328.
(21) Granucci, G.; Hynes, J. T.; Millié, P.; Tran-Thi, T.-H. *J. Am. Chem. Soc.* **2000**, *122*, 12243.
(22) Kiefer, P. M.; Hynes, J. T. *J. Phys. Chem. A* **2002**, *106*, 1834.
(23) Laage, D.; Burghardt, I.; Sommerfeld, T.; Hynes, J. T. *ChemPhysChem* **2003**, *4*, 61.
(24) Pines, E. In *The Chemistry of Phenols*; Rappoport, Z., Ed.; Wiley: Chichester, UK, 2003; Chapter 7.
(25) Agmon, N.; Rettig, W.; Groth, C. *J. Am. Chem. Soc.* **2002**, *124*, 1089.
(26) Solntsev, K. M.; Huppert, D.; Tolbert, L. M.; Agmon, N. *J. Am. Chem. Soc.* **1998**, *120*, 7981.
(27) Tolbert, L. M.; Haubrich, J. E. *J. Am. Chem. Soc.* **1994**, *116*, 10593.
(28) Fillingim, T. G.; Luo, N.; Lee, J.; Robinson, G. W. *J. Phys. Chem.* **1990**, *94*, 6368.
(29) Pines, E.; Fleming, G. R. *J. Phys. Chem.* **1991**, *95*, 10448.
(30) Knochenmuss, R.; Solntsev, K. M.; Tolbert, L. M. *J. Phys. Chem. A* **2001**, *105*, 6393.
(31) Kotlyar, A. B.; Borovok, N.; Kiryati, S.; Nachliel, E.; Gutman, M. *Biochemistry* **1994**, *33*, 873.
(32) Bardez, E. *Isr. J. Chem.* **1999**, *39*, 319.
(33) Fang, W.-H. *J. Am. Chem. Soc.* **1998**, *120*, 7568.
(34) Kohtani, S.; Tagami, A.; Nakagaki, R. *Chem. Phys. Lett.* **2000**, *316*, 88.
(35) Coussan, S.; Bach, A.; Leutwyler, S. *J. Phys. Chem. A* **2000**, *104*, 9864.
(36) Bardez, E.; Fedorov, A.; Berberan-Santos, M. N.; Martinho, J. M. G. *J. Phys. Chem. A* **1999**, *103*, 4131.
(37) Bach, A.; Hewel, J.; Leutwyler, S. *J. Phys. Chem. A* **1998**, *102*, 10476.
(38) Lee, S.-I.; Jang, D.-J. *J. Phys. Chem.* **1995**, *99*, 7537.
(39) Kim, T.-G.; Lee, S.-I.; Jang, D.-J.; Kim, Y. *J. Phys. Chem.* **1995**, *99*, 12698.
(40) Bardez, E.; Chatelain, A.; Larrey, B.; Valeur, B. *J. Phys. Chem.* **1994**, *98*, 2357.
(41) Bardez, E.; Devol, I.; Larrey, B.; Valeur, B. *J. Phys. Chem. B* **1997**, *101*, 7786.
(42) Mason, S. F.; Philp, J.; Smith, B. E. *J. Chem. Soc. A* **1968**, 3051.
(43) Poizat, O.; Bardez, E.; Buntinx, G.; Alain, V. *J. Phys. Chem. A* **2004**, *108*, 1873.
(44) Yu, H.; Kwon, O.-H.; Jang, D.-J. *J. Phys. Chem. A* **2004**, *108*, 3970.
(45) García-Ochoa, I.; Díez López, M.-A.; Viñas, M. H.; Santos, L.; Martínez Ataz, E.; Sánchez, F.; Douhal, A. *Chem. Phys. Lett.* **1998**, *296*, 335.
(46) Mehata, M. S.; Joshi, H. C.; Tripathi, H. B. *Chem. Phys. Lett.* **2002**, *359*, 314.
(47) Meuwly, M.; Bach, A.; Leutwyler, S. *J. Am. Chem. Soc.* **2001**, *123*, 11446.
(48) Douhal, A.; Dabrio, J.; Sastre, R. *J. Phys. Chem.* **1996**, *100*, 149.
(49) Roberts, E. L.; Chou, P. T.; Alexander, T. A.; Agbaria, R. A.; Warner, I. M. *J. Phys. Chem.* **1995**, *99*, 5431.
(50) Douhal, A. *Acc. Chem. Rev.* **2004**, *37*, 349.

(51) Hansen, J. E.; Pines, E.; Fleming, G. R. *J. Phys. Chem*. **1992**, *96*, 6904.
(52) Douhal, A.; Amat-Guerri, F.; Acuňa, A. U. *Angew. Chem., Int. Ed.* **1997**, *36*, 1514.
(53) García-Ochoa, I.; Díez López, M.-A.; Viñas, M. H.; Santos, L.; Martínez-Ataz, E.; Amat-Guerri, F.; Douhal, A. *Chem. Eur. J.* **1999**, *5*, 897.
(54) Organero, J. A.; Douhal, A. *Chem. Phys. Lett*. **2003**, *373*, 426.
(55) Saenger, W. *Angew. Chem., Int. Ed. Engl*. **1980**, *19*, 344.
(56) Douhal, A. *Chem. Rev.* **2004**, *104*, 1955.
(57) Douhal, A.; Fiebig, T.; Chachisvilis, M.; Zewail, A. H. *J. Phys. Chem. A* **1998**, *102*, 1657.
(58) Bhattacharyya, K. *Acc. Chem. Res.* **2003**, *36*, 95.
(59) Nandi, N.; Bhattacharyya, K.; Bagchi, B. *Chem. Rev.* **2000**, *100*, 2013.
(60) Chou, P.-T.; Liu, Y.-I.; Wu, G.-R.; Shiao, M.-Y.; Yu, W.-S.; Cheng, C.-C.; Chang, C.-P. *J. Phys. Chem. B* **2001**, *105*, 10674.
(61) Knutson, J. R.; Beechem, J. M.; Brand, L.*Chem. Phys. Lett.* **1983**, *102*, 501.
(62) Baeyens, W. R. G.; de Keukeleire, D.; Korkidis, K. *Luminescence Techniques in Chemical and Biological Analysis*; Marcel Dekker: New York, 1991; Chapter 3.
(63) Pines, E.; Pines, D.; Barak, T.; Magnes, B.-Z.; Tolbert, L. M.; Haubrich, J. E. *Ber. Bunsen-Ges. Phys. Chem.* **1998**, *102*, 511.
(64) Pines, E.; Magnes, B.-Z.; Lang, M. J.; Fleming, G. R. *Chem. Phys. Lett.* **1997**, *281*, 413.
(65) Pines, E.; Tepper, D.; Magnes, B.-Z.; Pines, D.; Barak, T. *Ber. Bunsen-Ges. Phys. Chem.* **1998**, *102*, 504.
(66) Pines, E.; Fleming, G. R. *Chem. Phys.* **1994**, *183*, 393.
(67) Calculated with the average of absorption and fluorescence using the Förster equation.[9]
(68) Bell, R. L.; Truong, T. N. *J. Phys. Chem. A* **1997**, *101*, 7802.
(69) Chou, P.-T.; Yu, W.-S.; Wei, C.-Y.; Cheng, Y.-M.; Yang, C.-Y. *J. Am. Chem. Soc*. **2001**, *123*, 3599.
(70) Solntsev, K. M.; Huppert, D.; Agmon, N.; Tolbert, L. M. *J. Phys. Chem. A* **2000**, *104*, 4658.